8-15-2006

The active FMR1 promoter is associated with a large domain of altered chromatin conformation with embedded local histone modifications

Nele Gheldof
University of Massachusetts Medical School

Tomoko M. Tabuchi
University of Massachusetts Medical School, tomoko.tabuchi@umassmed.edu

Job Dekker
University of Massachusetts Medical School, Job.Dekker@umassmed.edu

The active FMR1 promoter is associated with a large domain of altered chromatin conformation with embedded local histone modifications

Nele Gheldof, Tomoko M. Tabuchi, and Job Dekker*

Program in Gene Function and Expression and Department of Biochemistry and Molecular Pharmacology, University of Massachusetts Medical School, 364 Plantation Street, Worcester, MA 01605

Communicated by Nancy Kleckner, Harvard University, Cambridge, MA, June 26, 2006 (received for review May 9, 2006)

We have analyzed the effects of gene activation on chromatin conformation throughout an ≈170-kb region comprising the human fragile X locus, which includes a single expressed gene, FMR1 (fragile X mental retardation 1). We have applied three approaches: (*i*) chromosome conformation capture, which assesses relative interaction frequencies of chromatin segments; (*ii*) an extension of this approach that identifies domains whose conformation differs from the average, which we developed and named chromosome conformation profiling; and (*iii*) ChIP analysis of histone modifications. We find that, in normal cells where FMR1 is active, the FMR1 promoter is at the center of a large (≈50 kb) domain of reduced intersegment interactions. In contrast, in fragile X cells where FMR1 is inactive, chromatin conformation is uniform across the entire region. We also find that histone modifications that are characteristic of active genes occur tightly localized around the FMR1 promoter in normal cells and are absent in fragile X cells. Therefore, the expression-correlated change in conformation affects a significantly larger domain than that marked by histone modifications. Domain-wide changes in interaction probability could reflect increased chromatin expansion and may also be related to an altered spatial disposition that results in increased intermingling with unrelated loci. The described approaches are widely applicable to the study of conformational changes of any locus of interest.

chromatin domain | chromosome conformation capture | transcription | fragile X locus

Gene expression is associated with alterations in chromatin structure, both at the nucleosome level and at the level of larger chromatin domains. Whereas modification at the nucleosome level has been studied in detail, conformational changes of larger domains in relation to gene expression are much less understood, in part because of technical challenges to the study of chromatin at the level of tens of kilobases.

Active genes are marked by acetylation of histones H3 and H4 and by methylation of H3 at lysine 4 (H3K4). Recent studies have shown that these modifications occur in a punctate fashion at or near transcription start sites (1, 2). Promoter regions of active genes are also characterized by changes in chromatin accessibility, as exemplified by formation of DNase I hypersensitive sites (3).

In several cases, gene activation is accompanied by large-scale changes in chromatin conformation. First, activation or repression of genes can involve formation of chromatin loops through long-range interactions between regulatory elements (4–8). Second, activation of gene clusters can be accompanied by large-scale chromatin decondensation. For instance, upon activation of the β-globin locus, the entire ≈120-kb gene cluster becomes more accessible to nucleases, suggesting that chromatin throughout the locus is less condensed (9). Similarly, induction of arrays of multiple copies of reporter genes resulted in formation of extended chromatin fibers (10, 11). Decondensation is often associated with movement of the locus to the edge of the main chromosome mass or "territory." For example, activation of the HoxB cluster was associated with domain-wide decondensation and a change in nuclear position so that the genes loop out of the bulk of the chromosome (12).

In all of the cases analyzed thus far for long-range effects, the affected loci comprise large gene clusters. Whether such changes are general characteristics of gene expression at all types of loci is not known. In addition, relationships between any of these changes and histone modifications are poorly understood.

To address these issues, we studied the human fragile X locus, which provides a simple model system for analysis of chromatin conformation in relation to expression of an individual gene. This locus contains the FMR1 (fragile X mental retardation 1) gene, which is regulated as a single independent unit and can be studied in two opposite expression states: In healthy individuals, FMR1 is expressed; in fragile X patients, it is silenced. Silencing of FMR1 is caused by expansion of a CGG trinucleotide repeat located in the first exon of the gene (13). This genetic alteration triggers DNA methylation of the repeat plus local changes in histone modifications (14–16). When combined, these epigenetic alterations induce the silencing of FMR1, leading to the clinical features of fragile X syndrome, the most common form of inherited mental retardation (17).

Previous studies have focused on analysis of local chromatin modifications of the ≈2 kb immediately surrounding the FMR1 promoter. The active promoter displays high levels of histone acetylation and H3K4 methylation, whereas the silenced promoter is enriched in H3K9 methylation (14–16). Further, expression of FMR1 was correlated with formation of DNaseI hypersensitive sites at the promoter, pointing to an open chromatin conformation at this site (18). However, these studies did not address the possibility of larger-scale modifications of either histone modifications or general chromatin conformation.

Here, we used chromosome conformation capture (3C) to assess chromatin conformation around FMR1, in relation to its expression status, over distances of up to ≈80 kb on either side. This approach allows analysis of chromatin conformation at a scale of tens of kilobases (19). Changes at this scale are typically too small to be detectable by microscopic methods. We find that the promoter of the expressed FMR1 gene forms the midpoint of a large (≈50 kb) chromatin domain that is characterized by intersegment interaction frequencies that are generally lower than those in flanking chromatin. We further find that H3 acetylation and H3K4 methylation are mainly localized at the center of this domain, coincident with the 5′ end of the gene, whereas H4 acetylation is more spread out, particularly toward the 3′ end of the gene. None of these features is present when FMR1 is silenced. Our findings suggest that

Conflict of interest statement: No conflicts declared.

Abbreviations: 3C, chromosome conformation capture; CCP, chromosome conformation profiling.

*To whom correspondence should be addressed. E-mail: job.dekker@umassmed.edu.

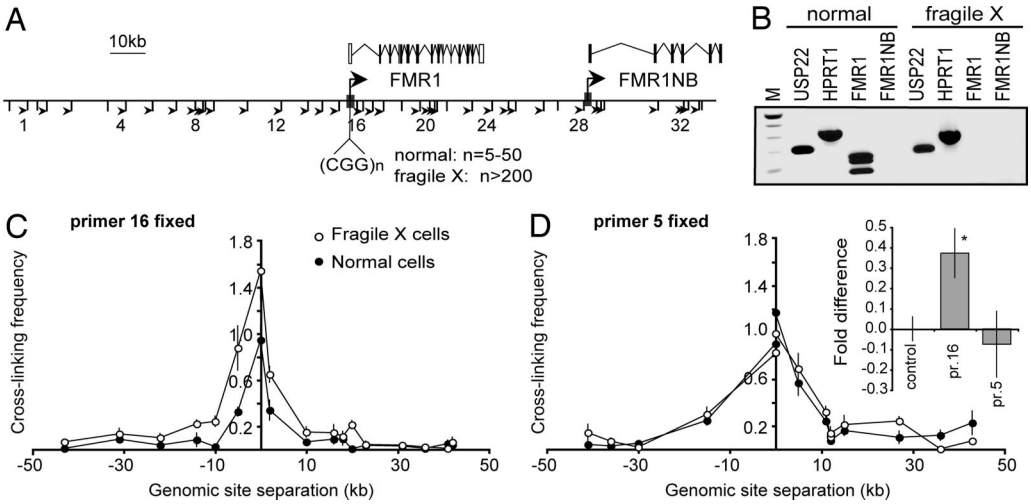

Fig. 1. 3C analysis of the fragile X locus. (*A*) Map of the 170-kb fragile X locus located on the X chromosome. The location of the CGG repeat in FMR1 is indicated. Hatch marks, EcoRI sites; arrowheads, location of 3C primers; large arrows, transcription start sites; gray boxes, CpG islands. (*B*) RT-PCR analysis of USP22, HPRT1, FMR1, and FMR1NB transcription in normal and fragile X cells. The different sizes of the FMR1 transcripts are due to alternative splicing. (*C*) Analysis of interactions between the FMR1 promoter (primer 16) and fragments up- and downstream in normal cells (filled circles) and fragile X cells (open circles). Vertical bars indicate standard error of the mean ($n = 3$). (*D*) Analysis of interactions between an EcoRI fragment located 60 kb upstream of the FMR1 promoter (primer 5) and surrounding fragments. (*Inset*) The fold difference (average log ratio) of (normalized) interaction frequencies in fragile X cells compared with normal cells in the control locus (USP22) and the regions around fragments 16 and 5 in the fragile X locus. A 2.4-fold difference in interaction frequencies is observed in the region around the promoter (primer 16) (*, $P < 0.05$), but no significant difference is observed in the upstream region (primer 5).

transcription-correlated histone modifications are relatively local effects, embedded within a larger domain of altered chromatin conformation.

Results

We analyzed chromatin conformation of the human FMR1 gene (Fig. 1*A*) by using two EBV-transformed lymphoblastoid cell lines in which FMR1 is either expressed (GM01989, normal cells) or silenced because of a CGG trinucleotide repeat expansion (GM3200, fragile X cells). The FMR1NB gene, located 30 kb downstream of FMR1, is not expressed in either cell line (Fig. 1*B*).

We studied chromatin conformation by using 3C (19). 3C is used to determine relative probabilities of interaction for pairs of segments that, when combined, reflect the spatial conformation of chromatin. In the 3C methodology, formaldehyde treatment cross-links proteins to DNA and to other proteins, which results in covalent linkage of interacting chromatin segments throughout the genome. Interactions between pairs of segments are then detected and quantified through a series of steps involving restriction digestion, intramolecular ligation, and PCR (see *Materials and Methods* and refs. 8 and 19–23).

Chromatin Conformation Around the FMR1 Promoter Is Correlated with Expression. We first tested whether activation or repression of FMR1 involves specific, long-range looping interactions between the FMR1 promoter and distant elements. We determined interaction frequencies in normal cells between the EcoRI fragment that overlaps with the FMR1 promoter and EcoRI fragments located throughout an 80-kb region surrounding the promoter. We found that the promoter interacted frequently with neighboring fragments but that interaction frequencies rapidly decreased for fragments that were located at larger genomic distances (Fig. 1*C*). This inverse relationship between interaction frequency and genomic site separation is similar to what has been observed in yeast and mouse cells (5, 19) and is the pattern expected for a linear chromatin fiber (23, 24). These results indicate the absence of specific looping interactions between the FMR1 promoter and segments located within 40 kb on either side of the promoter.

We performed the same analysis in fragile X cells. We found that the inactive FMR1 gene also displays a linear conformation that corresponds closely to that observed for the active FMR1 gene (Fig. 1*C*).

To permit direct quantitative comparison of data obtained in normal and fragile X cells, interaction frequencies must first be normalized to a common standard. To that end, we determined 47 interaction frequencies around the ubiquitously expressed USP22 (ubiquitin-specific protease 22) gene in both cell lines and used this data set for normalization (see *Materials and Methods*). Interestingly, inspection of the normalized data reveals that all interaction frequencies between the FMR1 promoter and fragments located up to 30 kb away on either side are significantly lower in cells where FMR1 is expressed compared with cells where FMR1 is silenced (Fig. 1 *C* and *D*).

We wished to determine whether this difference is specific for the FMR1 promoter. Therefore, we analyzed interaction frequencies between an EcoRI fragment located 60 kb upstream of the FMR1 promoter and its surrounding chromatin. Again, we find an inverse relationship between interaction frequency and genomic site separation. In contrast to the promoter region, however, the upstream region does not exhibit any significant differences in normalized interaction frequencies in normal and fragile X cells (Fig. 1*D*). We conclude that the conformation of a region around the FMR1 promoter is correlated with the expression status of FMR1, whereas a region located ≈60 kb upstream is not affected.

Chromosome Conformation Profiling (CCP) of the Fragile X Locus. The analysis described above suggests that chromatin domains can differ in average frequency of interaction among the DNA segments contained within them. To further confirm and analyze the existence of a domain with low interaction frequencies around the active FMR1 promoter, we devised the CCP strategy. CCP specifically identifies the locations and sizes of chromatin domains whose 3C interaction frequencies are either higher or lower than that of "average" chromatin.

CCP involves four steps. First, 3C interaction frequencies are determined for pairs of segments throughout a chromosomal

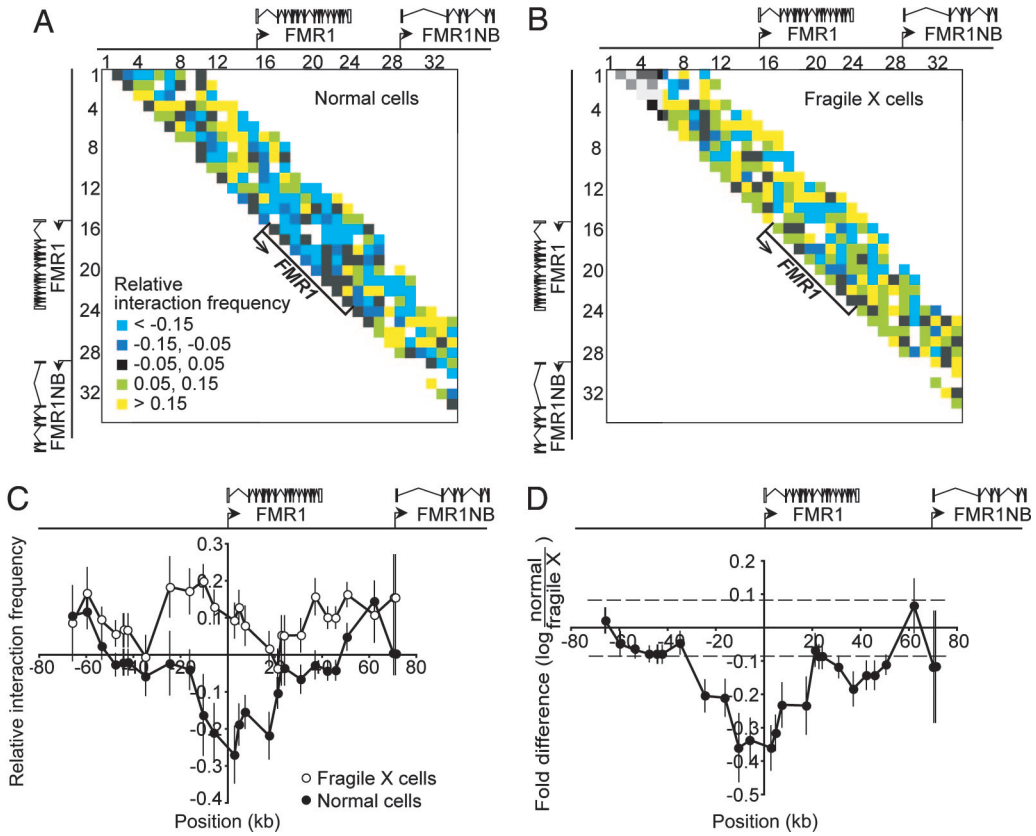

Fig. 2. CCP of the fragile X locus. (*A* and *B*) Schematic representations of relative interaction frequencies (see *Results*) throughout the fragile X locus for sites separated by up to 50 kb in normal cells (*A*) and fragile X cells (*B*). Each relative interaction frequency was assigned a color depending on whether it was higher than (yellow hues), equal to (black), or lower than (blue hues) zero. Numbers above and left of the matrix refer to 3C primers (Fig. 1*A*). (*C*) Moving average of relative interaction frequencies determined with a 30-kb sliding window through the matrices in *A* and *B* (filled circles, normal cells; open circles, fragile X cells). A value of zero on the *x* axis corresponds to the transcriptional start site of the *FMR1* gene. Vertical bars indicate standard error of the mean. (*D*) Fold change in relative interaction frequencies in fragile X cells versus normal cells along the fragile X locus. For each pair of fragments, the fold difference (log ratio) in interaction frequency in fragile X cells versus normal cells was calculated. The moving average of the fold difference is plotted by using a 30-kb sliding window. Horizontal dashed lines indicate the 95% confidence interval based on the error in data normalization (two times the standard error of the normalization factor). Points above the higher line or below the lower line are considered significantly different in normal cells versus fragile X cells.

region of interest. Second, for each intersegment separation distance (in kilobases), the region-wide average interaction frequency for all assayed segment pairs is determined. Third, for each interaction frequency, it is determined whether the value is higher or lower than the locus-wide average for the corresponding genomic site separation by calculation of the log ratio of the two frequencies. This log ratio is referred to as the relative interaction frequency. Fourth, relative interaction frequencies for all segment pairs are presented as a color-coded matrix in which each square represents a single pair. The data can then be subjected to sliding window analysis to determine whether relatively high or relatively low interaction frequencies are enriched in particular genomic regions.

We applied CCP to analysis of a 170-kb region around the FMR1 gene. We carried out 3C with a set of 34 primers spread throughout the region around FMR1 (Fig. 1*A*). We determined a total of 366 interaction frequencies between pairs of segments located throughout this region in both normal cells and fragile X cells. The two data sets were normalized to one another by using the set of 47 interactions determined around the USP22 locus as described above. Plots of normalized interaction frequencies as a function of intersegment distance again reveal that interaction frequencies rapidly decrease with increasing genomic distance (Fig. 5, which is published as supporting information on the PNAS web site) with no pronounced peaks in interaction frequency detectable, thus confirming that the entire locus displays a linear conformation (23). Calculation of relative interaction frequencies in both cell lines by using the locus-wide averages determined in normal cells as described above yields a pair of corresponding matrices: one for normal cells (Fig. 2*A*) and one for fragile X cells (Fig. 2*B*). Visual inspection of the data from normal cells reveals the presence of a large (≈50 kb) domain around the 5′ end of the FMR1 gene where almost all relative interaction frequencies are below the average and where, in the flanking domains, relative interaction frequencies are higher. In contrast, this large domain appears absent in fragile X cells. These results point to the presence of an ≈50-kb domain of altered chromatin conformation specifically around the active FMR1 promoter.

Next, we determined the moving average of relative interaction frequencies throughout the locus by using sliding window analysis. We chose to use a 30-kb window, primarily because this size is the smallest for which each window contains a sufficient number of data points to permit detection of significant differences between regions. The results are presented in Fig. 2*C*. In normal cells, we again observe an ≈50-kb region in which the average relative interaction frequencies are significantly lower (50%) than in the surrounding chromatin ($P < 0.01$). Within this region, the lowest relative interactions occur around the 5′ end of FMR1. In fragile X cells, in contrast, the domain that is characterized by low interaction frequencies is not detected. Instead, we observe that relative interaction frequencies are

more even throughout the locus (no significant difference between the 50-kb domain around the promoter and flanking domains; $P = 0.17$).

Sliding window analysis tends to smooth data, which may result in overestimation of the size of the domain with altered interaction frequencies. To further examine domain boundaries, we inspected the subset of relative interaction frequencies that involve only directly neighboring segments. In normal cells, we find that interactions between neighbors are all below average throughout an ≈50-kb domain around the promoter and that, in fragile X cells, all of these interactions are higher than the average observed in normal cells (Fig. 2 *A* and *B*).

To define the region that displays differential chromatin interactions in the active and repressed locus in yet another way, we calculated for each individual pair of restriction fragments the fold difference in interaction frequency in normal cells versus fragile X cells. We then used a 30-kb sliding window to determine the moving average of the fold difference in interaction frequency throughout the 170-kb analyzed region (Fig. 2*D*). We find that interaction frequencies are significantly decreased in FMR1-expressing cells compared with fragile X cells throughout an ≈50-kb domain, and most strongly so at the FMR1 promoter, whereas they are not significantly different in flanking domains. This analysis also reveals that a region around the 3′ end of the expressed FMR1 gene displays reduced interaction frequencies compared with the silent locus.

3C Controls. Because 3C is based on formaldehyde cross-linking of proteins to DNA and to other proteins, a lower (or higher) than average probability of cross-linking in a particular region could reflect a lower (or higher) protein density rather than any difference in relative proximity. We performed the following analyses to estimate protein density throughout the fragile X locus.

First, because the most abundant proteins of chromatin are the histones, we assessed histone density by ChIP with antibodies to H3. We analyzed both normal and fragile X cells and detected no significant differences throughout the region in either cell line (Fig. 3*A*). These results imply that nucleosome density is homogeneous throughout the locus and does not significantly decrease around the active FMR1 when lower intersegment interaction frequencies are detected by 3C.

Second, we reasoned that differences in protein density should affect the number of proteins that become cross-linked to DNA, which in turn will determine the efficiency with which cross-linked chromatin can be digested with a restriction enzyme. In that case, genomic regions with high protein density should display a higher efficiency of cross-linking and a lower efficiency of digestion compared with regions with lower protein density. We determined digestion efficiency of cross-linked chromatin by PCR across EcoRI restriction sites. We find that, on average, ≈25% of each site cannot be digested, presumptively because of cross-linking of proteins to the restriction site (Fig. 3*B*). Further, and most importantly, in normal cells, we did not observe differences in digestion efficiency between EcoRI sites around the FMR1 promoter compared with those located in up- and downstream regions, nor did we observe any differences between normal and fragile X cells. We infer that the efficiency of cross-linking is very similar throughout the fragile X locus in both normal and fragile X cells.

Third, we considered whether the size of restriction fragments could affect their interaction frequency as detected by 3C. We plotted the relative interaction frequency versus the sum of the size of each pair of restriction fragments (Fig. 6, which is published as supporting information on the PNAS web site). We did not find a significant correlation, which suggests that, within the range of segment sizes used for our 3C analysis (0.4–16 kb), cross-linking efficiency is not significantly affected by restriction fragment size. In any case, any such bias would have been identical in the two cell lines and thus would not explain the difference in interaction frequencies observed between the two FMR1 expression states.

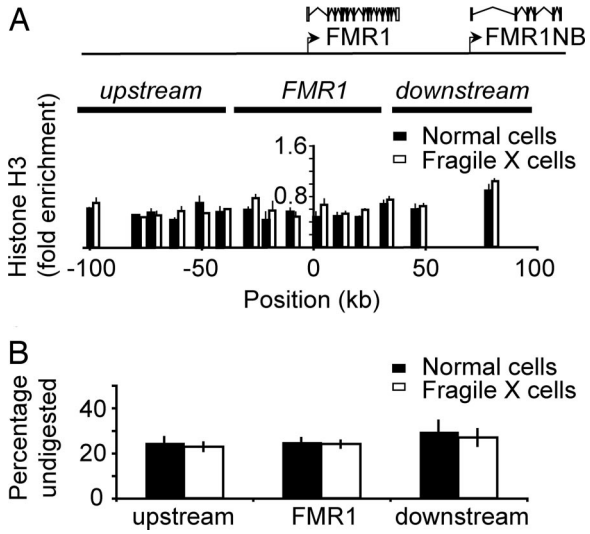

Fig. 3. Differences in interaction frequencies are not due to differential protein density. (*A*) Distribution of histone H3 across the fragile X locus in normal cells (filled bars) and fragile X cells (open bars) as determined by ChIP. (*B*) EcoRI digestion efficiency of cross-linked chromatin was calculated as the ratio of undigested to digested material in the three regions of the fragile X locus (indicated in *A*) in normal cells (filled bars) and fragile X cells (open bars). For each region, digestion efficiency of four EcoRI sites was determined in triplicate.

These control experiments suggest that reduced 3C cross-linking efficiencies around the active FMR1 promoter are not due to extraneous effects but do truly reflect lower relative intersegment interaction probabilities.

Histone Modifications Are Mainly Restricted to the FMR1 Promoter. Previous studies have analyzed histone modifications in only a small (≈2 kb) region around the FMR1 promoter (14–16). In light of the findings presented above, we were interested in determining the relationship between histone modifications and the region of altered chromatin conformation detected by 3C. We examined histone modification status throughout the ≈170-kb locus analyzed by CCP above. We carried out ChIP assays with antibodies to H3Ac, H4Ac, H3K4Me2, and H3K9Me2, followed by PCR with primer pairs designed approximately every 10 kb throughout the region (Fig. 4).

In normal cells, we observed high levels of H3Ac, H4Ac, and H3K4Me2 at the transcription start site of FMR1. High levels of H4Ac were also observed toward the 3′ end of the FMR1 gene. Histone modification levels were low throughout the rest of the fragile X locus. The promoter was also depleted for H3K9Me2, a modification that is correlated with inactive chromatin and that occurred at low levels throughout the locus. In fragile X cells, H3Ac, H4Ac, and H3K4Me2 at the FMR1 promoter were all reduced, whereas H3K9Me2 was increased at the transcription start site of FMR1, consistent with previous results (15).

Based on these results, we conclude that most histone modifications occur in a highly localized fashion at the transcription start site. H4Ac displayed a somewhat wider distribution, marking the 3′ end of the FMR1 gene as well.

Discussion

We find that the expressed and repressed states of the FMR1 gene display different chromatin conformations. The difference

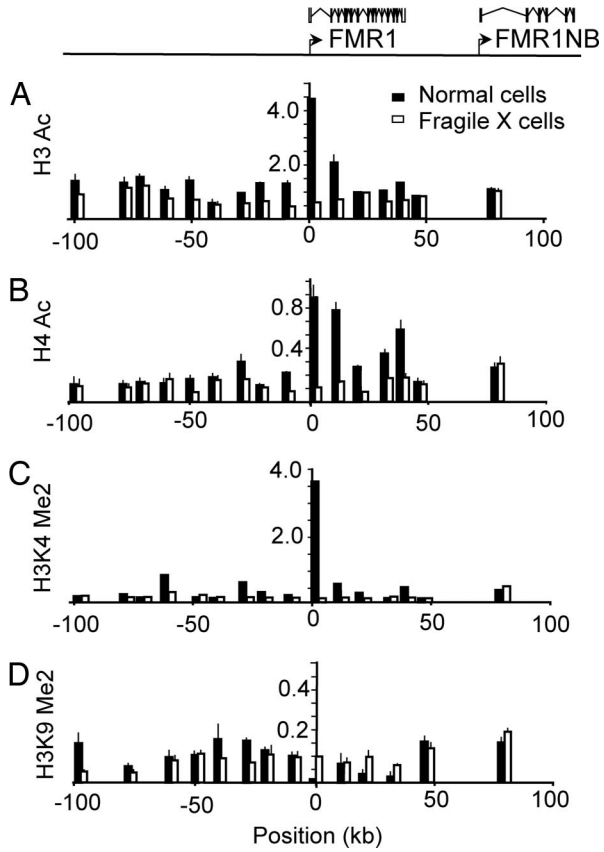

Fig. 4. Histone modification patterns of the fragile X locus as determined by ChIP. (*A*) Distribution of H3 acetylation across the fragile X locus in normal cells (filled bars) and fragile X cells (open bars). (*B*) H4 acetylation. (*C*) H3K4 dimethylation. (*D*) H3K9 methylation.

in conformation is reflected by a tendency for chromatin segments located throughout a 50-kb domain around the promoter to interact among each other less frequently when FMR1 is expressed compared with when the gene is repressed. To quantify and localize these differences, we developed CCP, a general tool that can be used to identify differences in average regional interaction frequencies along otherwise linear genomic regions. The most striking differences in interaction frequencies in the active locus compared with the repressed locus are observed throughout an ≈50-kb domain centered on the FMR1 promoter, but smaller differences can also be observed toward the 3′ end of the gene. The size of the domain that displays differential conformation is larger than the region marked by histone modifications, such as H3Ac and H3K4Me2, which occur specifically at the promoter. The fact that both the histone modifications and the domain-wide changes in chromatin conformation are centered on the active promoter suggests that these changes are nucleated by promoter activation. Below, we discuss possible models that can explain the formation of a large, structurally distinct chromatin domain.

Interpretation of 3C Data. Several different types of structural changes can explain the observed effects on chromatin interactions. One possible explanation appears to be ruled out. Given that 3C relies on formaldehyde cross-linking of proteins to DNA and to other proteins, lower interaction frequencies could be due to a change in protein density. However, we found no evidence that protein density is lower around the active promoter. We further note that, although it has recently been shown that gene activation can result in loss of one or a few nucleosomes at a promoter (25), such a local loss in histone density would not explain the observed reduction in interaction frequency throughout a domain as large as that described here.

Specific physical explanations can be considered by assuming chromatin to be a flexible polymer. In this context, regional differences in interaction frequencies can be attributed to changes either in flexibility or in mass density (i.e., the contour length of a given number of kilobases). Polymer models (19, 24) predict that interaction frequencies will decrease if chromatin becomes less flexible or if the mass density becomes lower (i.e., as the fiber becomes more extended). Correspondingly, the chromatin fiber of the 50-kb domain around the FMR1 promoter may be either less flexible or more extended when FMR1 is expressed compared with when it is repressed. In either case, this domain is expected to occupy a larger effective volume (i.e., to be expanded when FMR1 is expressed), as has been observed upon activation of gene clusters (10, 11).

Histone modifications around the FMR1 promoter may directly affect chromatin conformation. *In vitro* experiments of chromatin fibers have shown that histone acetylation reduces the ability of chromatin to form compact fibers (26, 27). Because histone modifications occur in a highly punctate fashion at the FMR1 transcription start site, any conformational change induced by these modifications will be local. However, a local change in chromatin expansion at the FMR1 promoter may still affect interactions between a fragment located upstream of the promoter and one that is located downstream. Therefore, local histone modifications can contribute to at least some of the lower interaction frequencies that are observed around the promoter. Importantly, however, histone modifications at the promoter are unlikely to be the cause of observed reduced interaction frequencies between pairs of segments that are both located several kilobases up- or downstream of the promoter. Therefore, other factors must contribute to formation of the 50-kb domain of low interaction frequencies as well.

Recently, transcription-dependent repositioning of gene clusters has been observed by using microscopy. Specifically, active genes were found to frequently loop out of their chromosome territory and intermingle with other genes (12, 28, 29). These changes in subnuclear organization were correlated with formation of more expanded chromatin (29). Increased intermingling of a chromatin domain with unrelated loci would imply that segments within this domain now interact more frequently with other loci throughout the genome and thus less exclusively with one another, thereby leading to reduced intradomainal intersegment interactions. Therefore, we are intrigued by the possibility that the observed domain of lower interaction frequencies around the active FMR1 promoter may in part be the result of increased intermingling of this domain with other loci throughout the genome.

Local Versus Domainal Changes in Chromatin Conformation. All histone modifications analyzed in this work, except H4Ac, occur in a highly localized fashion around the FMR1 transcription start site. Thus, histone modification changes that are thought to be diagnostic of active genes occur over much shorter distances than the longer-range chromatin structural changes observed here. It will be interesting to determine whether this same differential pattern is observed at all expressed loci. On the other hand, H4Ac displayed a wider distribution and was also prominent at the 3′ end of FMR1, where (smaller) chromosome structural changes were also detected by CCP, suggesting that H4 acetylation could play a role in modification of large-scale chromatin structure. Interestingly, modification of H4 has been directly implicated in regulating the level of chromatin compaction (27, 30). The cause-and-effect relationships among promoter activation, local histone modifications, and broader domainal changes

remain to be determined. The CCP approach provides a widely applicable tool for studying these phenomena in detail.

Materials and Methods

Cell Culture. EBV-transformed lymphoblastoid cell lines were obtained from Coriell Cell Repositories (Camden, NJ). GM3200 carrying a fully methylated FMR1 allele with 530 CGG repeats was derived from a 34-year-old male fragile X patient (15). GM01989 was derived from a 33-year-old unaffected male. Cell lines were cultured in RPMI medium 1640 supplemented with L-glutamine/10% FBS/1% penicillin-streptomycin.

RT-PCR. Total RNA was isolated by using the RNeasy Mini Kit (Qiagen, Valencia, CA). cDNA was synthesized by using the Omniscript reverse transcriptase protocol (Qiagen) with specific primers and then was amplified by PCR. Primer sequences for detection of USP22, FMR1, and FMR1NB are available on request. HPRT1 primers are described by Gibbs *et al.* (31) (primers 243 and 244).

3C Analysis. 3C was performed as described in ref. 19 with minor modifications as described by Miele *et al.* (22). A control PCR template was generated by digestion and random ligation of yeast artificial chromosome 209g4 containing the human FMR1 gene with 20 CGG repeats and ≈300 kb proximal and 150 kb distal from the FMR1 gene (32) and BAC RP11-746M containing the *USP22* gene. Primer sequences are available on request. 3C analyses were performed in three independent experiments, with each quantified at least in triplicate. For data normalization, interactions between fragments around the ubiquitously expressed USP22 gene on chromosome 17 were determined (Fig. 5). Interactions between fragments separated by up to 50 kb were used for normalization. Normalization was performed by calculating the log ratio of each interaction frequency measured in GM3200 cells over GM01989 cells.

EcoRI cutting efficiency was determined throughout the fragile X and control loci. Cells were fixed with 1% formaldehyde. Chromatin was solubilized, and one part was digested with EcoRI, as during the 3C protocol, and one part was not digested. After digestion, cross-links were reversed, and DNA was purified. PCR across restriction sites was performed to determine the fraction of each site that was protected against digestion. The cutting efficiency in the control locus was used to normalize data obtained from both cell lines.

ChIP. Polyclonal antibodies to H3Ac (catalog no. 06-599), H4Ac (catalog no. 06-598), H3K9Me2 (catalog no. 07-212), and H3K4Me2 (catalog no. 07-030) were obtained from Upstate Biotech (Charlottesville, VA), and an antibody to H3 (catalog no. ab1791) was obtained from Abcam (Cambridge, MA). ChIP was carried out as described by the supplier. Primer pairs were designed every 10 kb throughout the fragile X locus (primer sequences are available on request). To allow comparison of histone modification levels in the fragile X locus of the two cell lines, we normalized the relative enrichment of chromatin segments for each immunoprecipitation relative to data obtained for the USP22 locus (using five primer pairs in the USP22 gene). Results are expressed relative to the input template. ChIP analyses were performed in two independent experiments, with each quantified by PCR at least in triplicate.

We thank members of J.D.'s laboratory, Marian Walhout, Jason Perry, and Bart Deplancke for critical reading of the manuscript and Dr. D. L. Nelson (Baylor College of Medicine, Houston, TX) for kindly providing the yeast artificial chromosome 209g4 clone. This work was supported by National Institutes of Health Grant HG003143 and a Worcester Foundation grant (both to J.D.).

1. Roh, T. Y., Cuddapah, S. & Zhao, K. (2005) *Genes Dev.* **19,** 542–552.
2. Bernstein, B. E., Kamal, M., Lindblad-Toh, K., Bekiranov, S., Bailey, D. K., Huebert, D. J., McMahon, S., Karlsson, E. K., Kulbokas, E. J., III, Gingeras, T. R., *et al.* (2005) *Cell* **120,** 169–181.
3. Sabo, P. J., Hawrylycz, M., Wallace, J. C., Humbert, R., Yu, M., Shafer, A., Kawamoto, J., Hall, R., Mack, J., Dorschner, M. O., *et al.* (2004) *Proc. Natl. Acad. Sci. USA* **101,** 16837–16842.
4. Carter, D., Chakalova, L., Osborne, C. S., Dai, Y.-F. & Fraser, P. (2002) *Nat. Genet.* **32,** 623–626.
5. Tolhuis, B., Palstra, R. J., Splinter, E., Grosveld, F. & de Laat, W. (2002) *Mol. Cell* **10,** 1453–1465.
6. Murrell, A., Heeson, S. & Reik, W. (2004) *Nat. Genet.* **36,** 889–893.
7. Spilianakis, C. G. & Flavell, R. A. (2004) *Nat. Immunol.* **5,** 1017–1027.
8. Vakoc, C., Letting, D. L., Gheldof, N., Sawado, T., Bender, M. A., Groudine, M., Weiss, M. J., Dekker, J. & Blobel, G. A. (2005) *Mol. Cell* **17,** 453–462.
9. Bulger, M., Schubeler, D., Bender, M. A., Hamilton, J., Farrell, C. M., Hardison, R. C. & Groudine, M. (2003) *Mol. Cell. Biol.* **23,** 5234–5244.
10. Tumbar, T., Sudlow, G. & Belmont, A. S. (1999) *J. Cell Biol.* **145,** 1341–1354.
11. Muller, W. G., Walker, D., Hager, G. L. & McNally, J. G. (2001) *J. Cell Biol.* **154,** 33–48.
12. Chambeyron, S. & Bickmore, W. A. (2004) *Genes Dev.* **18,** 1119–1130.
13. Jin, P. & Warren, S. T. (2000) *Hum. Mol. Genet.* **9,** 901–908.
14. Coffee, B., Zhang, F., Warren, S. T. & Reines, D. (1999) *Nat. Genet.* **22,** 98–101.
15. Coffee, B., Zhang, F., Ceman, S., Warren, S. T. & Reines, D. (2002) *Am. J. Hum. Genet.* **71,** 923–932.
16. Pietrobono, R., Tabolacci, E., Zalfa, F., Zito, I., Terracciano, A., Moscato, U., Bagni, C., Oostra, B., Chiurazzi, P. & Neri, G. (2005) *Hum. Mol. Genet.* **14,** 267–277.
17. O'Donnell, W. T. & Warren, S. T. (2002) *Annu. Rev. Neurosci.* **25,** 315–338.
18. Eberhart, D. E. & Warren, S. T. (1996) *Somat. Cell Mol. Genet.* **22,** 435–441.
19. Dekker, J., Rippe, K., Dekker, M. & Kleckner, N. (2002) *Science* **295,** 1306–1311.
20. Dekker, J. (2003) *Trends Biochem. Sci.* **28,** 277–280.
21. Splinter, E., Grosveld, F. & de Laat, W. (2004) *Methods Enzymol.* **375,** 493–507.
22. Miele, A., Gheldof, N., Tabuchi, T. M., Dostie, J. & Dekker, J. (2006) in *Current Protocols in Molecular Biology*, eds. Ausubel, F. M., Brent, R., Kingston, R. E., Moore, D. D., Seidman, J. G., Smith, J. A. & Struhl, K. (Wiley, Hoboken, NJ), Suppl. 74, pp. 21.11.1–21.11-20.
23. Dekker, J. (2006) *Nat. Methods* **3,** 17–21.
24. Rippe, K. (2001) *Trends Biochem. Sci.* **26,** 733–740.
25. Sekinger, E. A., Moqtaderi, Z. & Struhl, K. (2005) *Mol. Cell* **18,** 735–748.
26. Tse, C., Sera, T., Wolffe, A. P. & Hansen, J. C. (1998) *Mol. Cell. Biol.* **18,** 4629–4638.
27. Shogren-Knaak, M., Ishii, H., Sun, J. M., Pazin, M. J., Davie, J. R. & Peterson, C. L. (2006) *Science* **311,** 844–847.
28. Volpi, E. V., Chevret, E., Jones, T., Vatcheva, R., Williamson, J., Beck, S., Campbell, R. D., Goldsworthy, M., Powis, S. H., Ragoussis, J., *et al.* (2000) *J. Cell Sci.* **113,** 1565–1576.
29. Branco, M. R. & Pombo, A. (2006) *PLoS Biol.* **4,** e138.
30. Dorigo, B., Schalch, T., Bystricky, K. & Richmond, T. J. (2003) *J. Mol. Biol.* **327,** 85–96.
31. Gibbs, R. A., Nguyen, P. N., McBride, L. J., Koepf, S. M. & Caskey, C. T. (1989) *Proc. Natl. Acad. Sci. USA* **86,** 1919–1923.
32. Peier, A. M., McIlwain, K. L., Kenneson, A., Warren, S. T., Paylor, R. & Nelson, D. L. (2000) *Hum. Mol. Genet.* **9,** 1145–1159.